

# Retardation and repair of fatigue cracks in a microcapsule toughened epoxy composite – Part I: Manual infiltration

E.N. Brown <sup>a,\*</sup>, S.R. White <sup>b</sup>, N.R. Sottos <sup>a</sup>

<sup>a</sup> Department of Theoretical and Applied Mechanics and the Beckman Institute for Advanced Science and Technology, University of Illinois at Urbana-Champaign, Urbana, IL 61801, USA

<sup>b</sup> Department of Aerospace Engineering and the Beckman Institute for Advanced Science and Technology, University of Illinois at Urbana-Champaign, Urbana, IL 61801, USA

Received 26 January 2005; received in revised form 19 April 2005; accepted 20 April 2005  
Available online 22 June 2005

## Abstract

As a first step towards a new crack healing methodology for cyclic loading, this paper examines two promising crack-tip shielding mechanisms during fatigue of a microcapsule toughened epoxy. Artificial crack closure is achieved by injecting precatalyzed monomer into the crack plane to form a polymer wedge at the crack tip. The effect of wedge geometry is also considered, as dictated by crack loading conditions during infiltration. Crack-tip shielding by a polymer wedge formed with the crack held open under the maximum cyclic loading condition ( $K_{max}$ ) yields temporary crack arrest and extends the fatigue life by more than 20 times. Hydrodynamic pressure and viscous damping as a mechanism of crack-tip shielding are also investigated by injecting mineral oil into the crack plane. Viscous fluid flow leads to retardation of crack growth independent of initial loading conditions. The success of these mechanisms for retarding fatigue crack growth demonstrates the potential for in situ self-healing of fatigue damage.

© 2005 Elsevier Ltd. All rights reserved.

**Keywords:** A. smart materials; A. polymer-matrix composites; B. fatigue; C. failure criterion; Self-healing

## 1. Introduction

Thermosetting polymers are used in a wide variety of applications ranging from structural composites to microelectronics. Due to low strain-to-failure, these polymers are highly susceptible to damage in the form of cracks. In structural composites these cracks can lead to fiber/matrix debonding and inter-ply delamination, ultimately resulting in component failure. Susceptibility to cyclic loading is particularly problematic because a crack will grow, however slowly, above a threshold

range of stress intensities  $\Delta K_{th}$  that is significantly lower than the critical stress intensity  $K_{IC}$ . Prevention of fatigue failure currently depends on accurate life prediction and implementation of inspection procedures.

Polymer fatigue has been studied extensively in both homogeneous and composite structures (e.g., [1–15]). In most polymers, fatigue crack growth rates ( $da/dN$ ) are accurately described by the Paris power law [16],

$$\frac{da}{dN} = C_0 \Delta K_I^n, \quad (1)$$

where  $C_0$  and  $n$  are material constants and  $\Delta K_I$  is the applied range of stress intensity. Typical Paris power law crack growth behavior is shown schematically by the solid curve in Fig. 1. Despite this understanding of cyclic crack growth, fatigue failure remains a major cause of component failure.

\* Corresponding author. Present address: Materials Science and Technology Division, Los Alamos National Laboratory, TA-35, Building 455, DCDP 01S, MS-E544, Los Alamos, NM 87545, USA. Tel.: +1 505 667 0799; fax: +1 505 667 2185.

E-mail address: [en\\_brown@lanl.gov](mailto:en_brown@lanl.gov) (E.N. Brown).

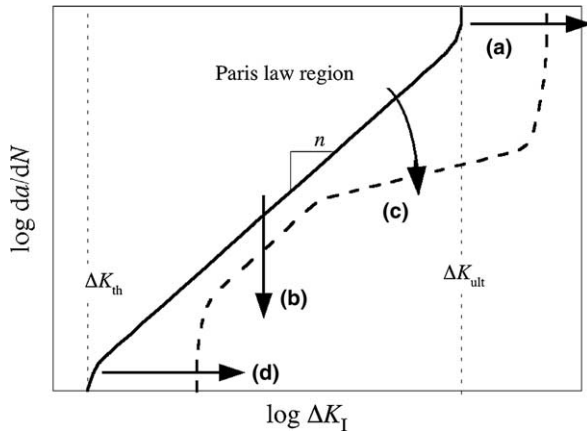


Fig. 1. Representative relationship between fatigue crack growth rate ( $da/dN$ ) and the applied stress intensity range ( $\Delta K_I$ ) in the Paris power law region. Improved fatigue behavior can be obtained by: (a) increasing the range of stress intensity before crack growth instability  $\Delta K_{ult}$ , (b) reducing the crack growth rate  $da/dN$  for a given  $\Delta K_I$ , (c) decreasing the crack growth rate sensitivity to  $\Delta K_I$ , i.e., reduce  $n$ , and (d) increasing the threshold  $\Delta K_{th}$  at which crack growth arrests.

Strategies for improving fatigue life are shown schematically in Fig. 1 and include: (a) increasing the range of stress intensity before crack growth instability  $\Delta K_{ult}$ , (b) decreasing the crack growth rate  $da/dN$  for a given  $\Delta K_I$ , (c) decreasing the crack growth rate sensitivity to  $\Delta K_I$ , i.e., reduce  $n$ , and (d) increasing the threshold  $\Delta K_{th}$  at which crack growth arrests. In the case of brittle thermosetting polymers, incorporation of a rubbery second phase [8–10], solid particles [11–13] or microcapsules [14,15] significantly improves fatigue performance by increasing the fracture toughness (Fig. 1(a)) and decreasing the Paris power law exponent (Fig. 1(c)). Of relevance for the current work, the presence of liquid-filled microcapsules increases the fracture toughness of epoxy by up to 127% [17]. The addition of microcapsules also significantly decreases the Paris power law exponent above a transition value of the stress intensity factor  $\Delta K_T$  [14]. In this regime, the Paris power law exponent decreases from approximately 10 for neat epoxy to 4.5 for concentrations above 10 wt% microcapsules.

In contrast to steady-state crack growth described by the Paris power law, many fatigue response mechanisms evolve over the course of loading, causing the fatigue crack growth rate to accelerate or decelerate under constant  $\Delta K_I$ . Crack-tip shielding mechanisms such as crack closure can significantly retard fatigue crack growth. Initial work on crack closure by Elber [18,19] is based on the development of a local plastic zone that shields the crack tip such that the crack tip stress state cannot unload beyond  $K_{closure}$  (Fig. 2(b)). This shielding mechanism leads to a local driving force for fatigue  $\Delta K_{eff}$  that is less than the applied  $\Delta K_I$ , and effectively reduces the crack growth rate.

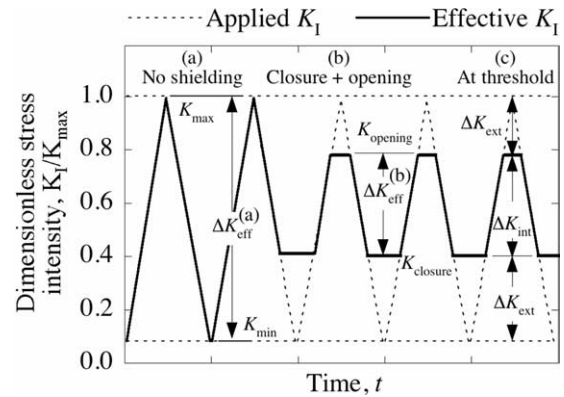


Fig. 2. Schematic of cyclic loading profile with crack-tip shielding nomenclature for three conditions: (a) no shielding ( $\Delta K_{eff} = \Delta K_I$ ), (b) shielding from crack closure preventing unloading to  $K_{min}$ , and (c) combined shielding from  $K_{max}$  and  $K_{min}$  (adapted from Shin et al. [23]).

More recently, artificial crack closure induced by infiltration of a polymer was reported to reduce constant  $\Delta K_I$  fatigue crack growth and increase the fatigue threshold in metals [20]. Cyclic loading was halted after the fatigue crack had grown significantly and an uncured polymer resin was injected into the crack plane. Once the resin cured, constant  $\Delta K_I$  cyclic loading was resumed. The presence of the polymer wedge prevented full unloading at the crack tip, increased the effective minimum value of the cyclic stress intensity (from  $K_{min}$  to  $K_{closure}$ ) and reduced the local driving force for fatigue  $\Delta K_{eff}$ , even though the applied  $\Delta K_I$  dictated by far-field loading was unchanged. Fatigue life-extensions from 100% [20,21] to 1000% [22,23] were observed with polymer infiltration. The cyclic loading profiles of the applied  $\Delta K_I$  and  $\Delta K_{eff}$  arising from the crack closure mechanism are illustrated schematically in Fig. 2(a) and (b) (adapted from [23]). Although Sharp et al. [22] proposed a further reduction of  $\Delta K_{eff}$  could be achieved by reducing the crack tip opening and thereby decreasing the effective maximum value of the cyclic stress intensity from  $K_{max}$  to  $K_{opening}$  (Fig. 2(c)), this mechanism led to negligible increases in fatigue life.

Hydrodynamic pressure crack-tip shielding due to viscous flow within a fatigue crack has also been reported to decrease the effective range of mode-I stress intensity and reduce fatigue crack growth rate [24,25]. These investigations were restricted to metals and performed with the specimens immersed in the fluid of interest. The forces required to squeeze a viscous fluid out of the crack during unloading and draw fluid into the crack during loading provided effective crack-tip shielding. Crack growth rates measured in oils were lower than in air. Greater reductions in crack growth rate occurred for higher viscosity oils [26–28], until an upper limit was reached and the fluid could no longer penetrate to the crack tip [29,30]. For metals, crack-tip shielding from hydrodynamic pressure provided nearly 50% reduction in crack growth rate [29,31].

In this work, we present a new methodology for retardation and repair of fatigue cracks based on the self-healing concept developed by White et al. [32]. In Part I we investigate two crack-tip shielding mechanisms during fatigue of a microcapsule toughened epoxy. Artificial crack closure is achieved by injecting precatalyzed monomer into the crack plane to form a polymer wedge at the crack tip. Hydrodynamic pressure and viscous damping at the crack tip are investigated by injecting mineral oil into the crack plane. Building on the success of these mechanisms for retarding fatigue crack growth, Part II [33] reports on in situ self-healing of fatigue damage.

## 2. Fatigue test method

### 2.1. Materials and sample preparation

Urea-formaldehyde microcapsules containing dicyclopentadiene (DCPD) monomer were manufactured with average diameter of 180  $\mu\text{m}$  using the emulsion in situ polymerization microencapsulation method outlined by Brown et al. [34]. Shell wall thickness was  $190 \pm 30$  nm for all batches. Tapered double-cantilever beam specimens were cast from EPON<sup>®</sup> 828 epoxy resin (DGEBA) and 12 pph Ancamine<sup>®</sup> DETA (diethylenetriamine) curing agent with 20 wt% of microcapsules mixed into the resin. For the work presented in this paper the effect of in situ self-healing was excluded by omitting the catalyst phase in the resin formulation. The epoxy mixture was degassed, poured into a closed silicone rubber mold and cured for 24 h at room temperature, followed by 24 h at 30 °C. Relevant physical and material properties are listed in Table 1.

### 2.2. Mechanical testing

The fatigue-crack propagation behavior of microcapsule toughened epoxy was investigated using the tapered double-cantilever beam (TDCB) specimen geometry, shown in Fig. 3. The fatigue experiment and specimen geometry are outlined by Brown et al. in [14] and [35], respectively. Side grooves are included to ensure controlled crack growth along the centerline of the brittle

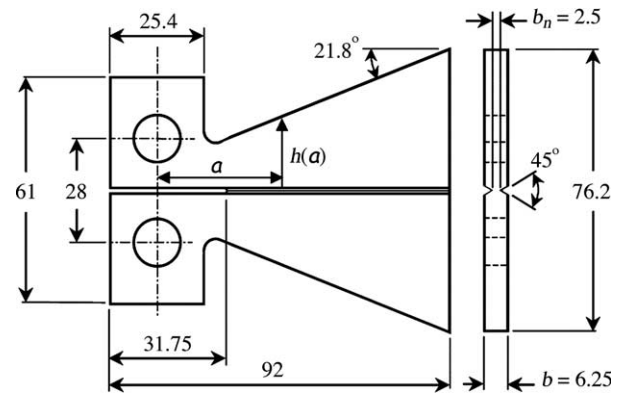


Fig. 3. Tapered-double-cantilever-beam geometry [35]. All dimensions in millimeters.

specimen. The TDCB geometry, developed by Mostovoy et al. [36], provides a crack-length-independent relationship between applied stress intensity factor  $K_I$  and load  $P$ ,

$$K_I = \alpha P, \quad (2)$$

which only requires knowledge of the coefficient  $\alpha = 11.2 \times 10^3 \text{ m}^{-3/2}$  [35]. A constant range of mode-I stress intensity factor  $\Delta K_I$  was achieved by applying a constant range of applied load  $\Delta P$ , independent of crack length.

Fatigue crack propagation studies were performed using an Instron DynoMight 8841 low-load frame with 250 N load cell. Samples were precracked with a razor blade while ensuring the precrack tip was centered in the groove and then pin loaded. A triangular waveform of frequency 5 Hz was applied with a load ratio ( $R = K_{\min}/K_{\max}$ ) of 0.1. Fatigue cracks were grown under mode-I stress intensity factor range  $\Delta K_I = 0.473 \text{ MPa m}^{1/2}$ . Crack lengths were measured optically and by specimen compliance [14]. First, the optically measured crack-tip position and specimen compliance were plotted against number of cycles. A linear relationship between crack length and specimen compliance was then used to calculate the crack-tip position at all times during the experiment.

The constant  $\Delta K$  nature of the fatigue test yields a constant crack-growth rate over the majority of the length of the specimen. The degree of observed crack acceleration fluctuates with loading conditions and

Table 1  
Properties of the constituent materials [14]

Property	Epoxy	Urea-formaldehyde microcapsules	Epoxy with 20 wt% microcapsules
$K_{IC}$ (MPa $\text{m}^{1/2}$ )	$0.55 \pm 0.04$	–	$1.0 \pm 0.2$
Young's modulus (GPa)	$3.4 \pm 0.1$	–	$2.7 \pm 0.1$
Paris power law exponent, $n$	9.7	–	4.3
Paris power law constant, $C_0$	$8.2 \times 10^{-2}$	–	$3.8 \times 10^{-4}$
Density (kg/ $\text{m}^3$ )	1160	~1000	~1120
Diameter ( $\mu\text{m}$ )	–	$180 \pm 40$	–
Wall thickness (nm)	–	$190 \pm 30$	–

sample material. In the absence of secondary shielding mechanisms, the rate is defined by the Paris power law dependence on the applied range of mode-I stress intensity factor  $\Delta K_I$  [14]. Any deviation during a given test (e.g., crack growth retardation or arrest) is therefore an isolated effect of either viscous flow or artificial crack closure. To account for the complexity associated with changing fatigue crack growth rates under cyclic loading conditions, fatigue-healing efficiency is defined by fatigue life-extension,

$$\lambda = \frac{N_{\text{healed}} - N_{\text{control}}}{N_{\text{control}}}, \quad (3)$$

where  $N_{\text{healed}}$  is the total number of cycles to failure for a self-healing sample and  $N_{\text{control}}$  is the total number of cycles to failure for a similar sample without healing.

### 3. Results

Healing under fatigue loading was first investigated by manual injection of pre-catalyzed healing agent in the crack plane (DCPD mixed with  $2 \text{ g L}^{-1}$  of Grubbs' first generation Ru catalyst). Healing agent was injected into the crack plane under three loading conditions: zero-load, constant  $K_{\text{max}}$ , and continuous cyclic loading. For a control experiment, a fatigue crack was grown in a sample without injection until failure occurred ( $N_{\text{control}} = 1.71 \times 10^5$  cycles). Infiltration of a viscous fluid (with no polymerization) was also explored for an additional comparison case.

For the zero-load case, a crack was grown for several millimeters at which point fatigue loading was interrupted, pre-catalyzed healing agent was injected into the crack plane, and all external loads were removed from the sample. Fatigue loading was reestablished after a 10 h healing (cure) period at room temperature. The crack-tip position is plotted against number of cycles for this case in Fig. 4. Following healing, the crack retreated to the approximate location of the sample pre-notch. Upon the resumption of cyclic loading, an interfacial crack rapidly initiated between the poly-DCPD and epoxy and propagated to the crack-tip position prior to healing. Crack growth in the neat epoxy commenced at its prehealed rate until sample failure. The fatigue-healing efficiency  $\lambda$  defined by Eq. (3) and calculated using the data from the control sample was less than 1%.

For the second loading case, a crack was grown for several millimeters, fatigue loading was interrupted, the sample was held at constant  $K_{\text{max}}$ , and pre-catalyzed healing agent was injected into the crack plane. Fatigue loading was reestablished after a 10 h healing period at room temperature. Crack-tip position is plotted against number of cycles for this case in Fig. 5. Crack growth through the polyDCPD region exhibited three regimes

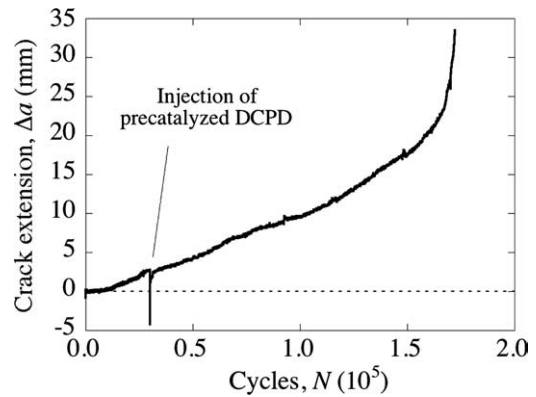


Fig. 4. Crack length vs. fatigue cycles of manual injection sample healed under zero-load and tested to failure,  $\lambda < 1\%$ .  $\Delta K_I = 0.473 \text{ MPa m}^{1/2}$ ,  $K_{\text{max}} = 0.525 \text{ MPa m}^{1/2}$ ,  $K_{\text{min}} = 0.053 \text{ MPa m}^{1/2}$ ,  $R = 0.1$ ,  $f = 5 \text{ Hz}$ , and  $a_0 = 24.3 \text{ mm}$ .

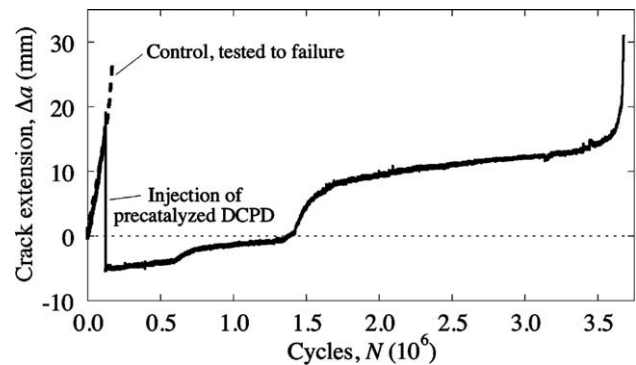


Fig. 5. Crack length vs. fatigue cycles of manual injection sample healed under  $K_{\text{max}}$  and control sample tested to failure,  $\lambda = 2052\%$ .  $\Delta K_I = 0.473 \text{ MPa m}^{1/2}$ ,  $K_{\text{max}} = 0.525 \text{ MPa m}^{1/2}$ ,  $K_{\text{min}} = 0.053 \text{ MPa m}^{1/2}$ ,  $R = 0.1$ ,  $f = 5 \text{ Hz}$ , and  $a_0 = 26.1 \text{ mm}$ .

of relatively stable crack-tip position. After significant life extension, crack growth in the toughened epoxy resumed at its prehealed growth rate. Sample failure of the healed specimen occurred after  $N_{\text{healed}} = 3.68 \times 10^6$  total applied cycles. For this case, the fatigue-healing efficiency  $\lambda$  defined by Eq. (3) was 2000%.

The load–displacement response changes significantly over the course of the sample fatigue life, shown in Fig. 6. In the early cycles, prior to injection of DCPD, the load–displacement relationship is linear with increasing compliance as the crack propagates. Following healing agent injection and polymerization at  $K_{\text{max}}$ , the load–displacement relationship remains linear with a reduced compliance. After numerous cycles without crack advance, the load–displacement curve becomes bimodal. The portion of the load–displacement curve above the knee becomes increasingly compliant as the crack length increases. Simultaneously, the knee occurs at decreasing load levels. Crack growth approaches the prehealed rate when the load–displacement curves return to a linear regime.

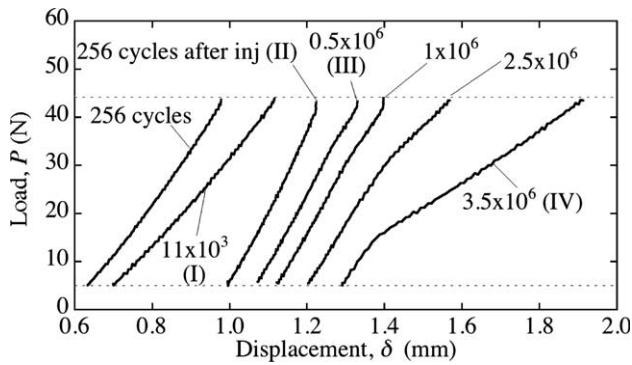


Fig. 6. Load–displacement curves for select cycles corresponding with Fig. 5.

For the continuous cyclic loading case, a crack was grown for several millimeters at which point precatalyzed healing agent was injected into the crack plane. The DCPD flowed backward and forward in the fracture plane corresponding to the closing and opening of the crack. The extent of flow decreased with time as the DCPD polymerized in the crack plane. Immediately following injection, the sample compliance decreased slightly and the crack arrested for the first 1.5 h following injection ( $2.7 \times 10^4$  cycles). Following gelation, the increased stiffness of the rubbery polymer appeared as a regression of the crack tip. Once the polyDCPD reached the glassy regime – characterized by the degree of cure for the glass transition temperature to exceed the ambient temperature [37] – the crack tip stabilized until debonding initiated. The fatigue life-extension  $\lambda$  associated with the temporary crack growth retardation shown in Fig. 7 was 56%.

For comparative purposes, infiltration of a non-healing viscous fluid was also investigated. A crack was grown for several millimeters in a microcapsule-tough-

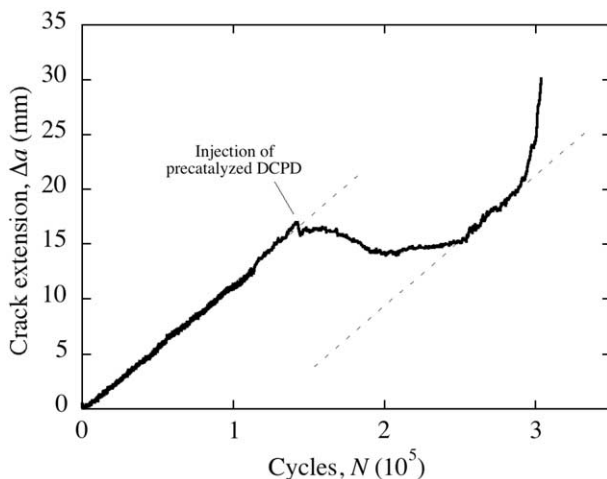


Fig. 7. Crack length vs. fatigue cycles of manual injection sample healed under continuous cyclic loading and tested to failure,  $\lambda = 55.9\%$ .  $\Delta K_I = 0.473 \text{ MPa m}^{1/2}$ ,  $K_{\max} = 0.525 \text{ MPa m}^{1/2}$ ,  $K_{\min} = 0.053 \text{ MPa m}^{1/2}$ ,  $R = 0.1$ ,  $f = 5 \text{ Hz}$ , and  $a_0 = 22.9 \text{ mm}$ .

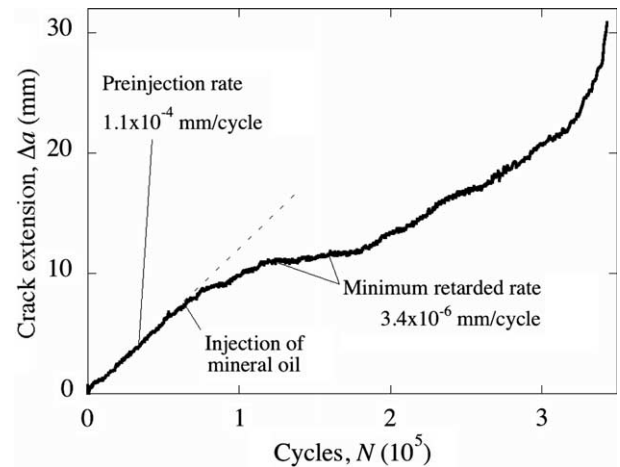


Fig. 8. Crack length vs. number of cycles for manual injection of mineral oil  $\lambda = 101\%$ . Hydrodynamic pressure from the viscous fluid dramatically reduces the crack growth rate and leads to significant life extension.  $\Delta K_I = 0.473 \text{ MPa m}^{1/2}$ ,  $K_{\max} = 0.525 \text{ MPa m}^{1/2}$ ,  $K_{\min} = 0.053 \text{ MPa m}^{1/2}$ ,  $R = 0.1$ ,  $f = 5 \text{ Hz}$ , and  $a_0 = 21.4 \text{ mm}$ .

ened epoxy sample and mineral oil (Fisher Scientific, New Jersey) was injected into the crack plane. Injection of mineral oil – an inert hydrocarbon oligomeric compound with a viscosity (30 cP at 40 °C) approximately 40 times higher than DCPD – dramatically reduced the crack growth rate (Fig. 8). Unlike the case of a submerged sample, where crack growth rates are reported to be steady [25], the retarded crack growth exhibited significant variability. Notably, crack growth retardation lagged the injection event, potentially due to the time required for the oil to be drawn into the crack tip. After a period of arrest, the crack growth rate increased (although never resuming the preinjection rate) in combination with an observed loss of oil from the crack plane.

#### 4. Discussion

Manual injection of precatalyzed monomer healing agent extends the fatigue life of microcapsule toughened epoxy through a combination of crack-tip shielding mechanisms. In samples injected with precatalyzed DCPD and healed at  $K_{\max}$ , crack closure due to the formation of a polyDCPD wedge at the crack tip provides the dominant shielding mechanism for fatigue crack retardation (Fig. 5). Conversely, the wedge polymerized at zero-load does not result in any crack-tip shielding through artificial crack closure (Fig. 4). As described previously for metals [21], a polymer wedge formed at or above  $K_{\max}$  provides maximum shielding efficiency and approaches a stress free crack tip. Shin et al. [23] have also reported that injection must occur at  $K_{\max}$  or larger to achieve any significant fatigue crack retardation.

The success of crack closure is strongly dependent on how efficiently the crack tip is shielded from the applied cyclic loads. The progression of the load–displacement curves in Fig. 6 is representative of crack closure and correlates well with the temporary crack arrest events observed in Fig. 5 following injection at  $K_{\max}$ . The stages of the crack closure mechanism are summarized schematically in Fig. 9. In the early cycles prior to injection of DCPD (Fig. 9(a) and (b)), the corresponding load–displacement curve in Fig. 6 (curve I) is linear with increasing compliance as the crack propagates. Following healing agent injection and cure (Fig. 9(c) and (d)), the load–displacement curve in Fig. 6 (curve II) remains linear with a reduced compliance due to the shorter, healed crack length. After numerous cycles without crack advance, the load–displacement curve becomes bimodal (Fig. 6, curve III), representative of the crack closure mechanism proposed by Elber [18]. The portion of the load–displacement curve above the knee, which represents the open crack condition and the portion of the cyclic load experienced by the crack tip, become increasingly compliant indicating progressive debonding of the healed DCPD interface as shown Fig. 9(e). The portion of the load–displacement curve below the knee, which represents the closed crack condition (Fig. 9(f)), retains a compliance corresponding to the healed crack geometry. Simultaneously, the knee occurs at decreasing loads, indicating an increase in the effective cyclic stress intensity at the crack tip. As the crack grows past the DCPD wedge (Fig. 9(g) and (h)), the crack growth rate

increases with increasing  $\Delta K_{\text{eff}}$  approaching the pre-healed rate and proceeds in this fashion until sample failure.

Hydrodynamic pressure at the crack tip associated with viscous healing agent in the crack plane also provides a shielding mechanism in microcapsule toughened epoxy. Injection experiments with both catalyzed healing agent (Fig. 7) and mineral oil (Fig. 8) demonstrate reduced crack growth rates. The effectiveness of DCPD at providing shielding by hydrodynamic pressure is dependent on the degree of cure ( $\alpha$ ). Low viscosity DCPD monomer ( $\alpha = 0$ ) has a low resistance to flow, providing nominal crack-tip shielding. As the degree of cure and viscosity increase, significant crack growth retardation is obtained. Further polymerization leads to crack regression as the shielding mechanism transitions from hydrodynamic pressure to crack closure.

The shielding effect of hydrodynamic pressure has been modeled analytically [29,30] and numerically [38] for fatigue crack growth in metals. As shown schematically in Fig. 10, the effective loading at a viscous fluid-filled crack tip lags behind and has a significantly different shape than the applied cyclic stress intensity profile. The models predict a reduction of crack growth rates for increased fluid viscosity, lower stress ratios  $R$ , lower applied ranges of stress intensity  $\Delta K_I$ , larger crack thickness  $b$ , and higher cyclic frequencies  $f$ . Because fatigue crack growth in metals is less sensitive to changes in  $\Delta K_I$  (Paris power law exponent  $n \sim 3$ ), partial shielding yields only a modest reduction in crack

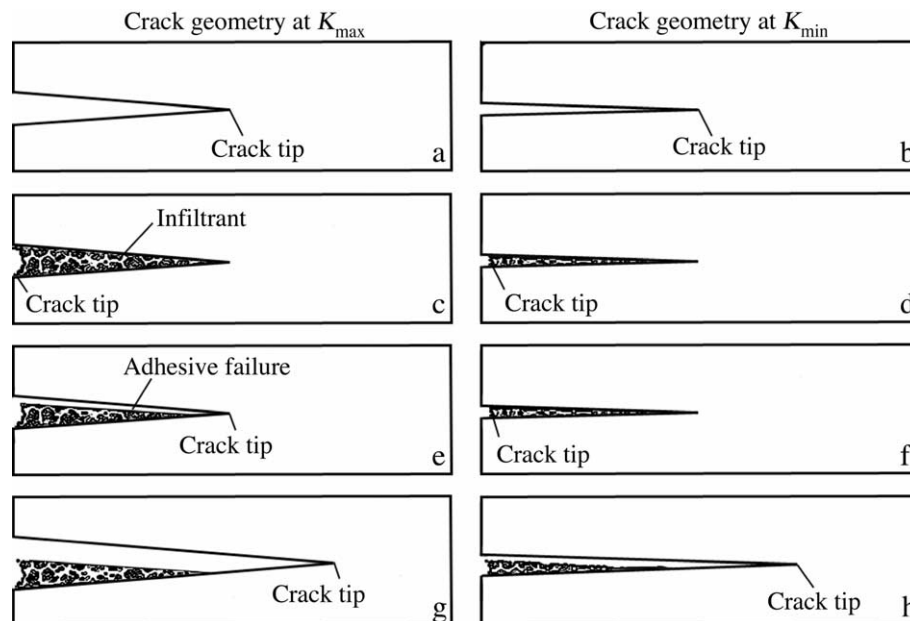


Fig. 9. Schematic summary of crack closure mechanism and the apparent crack-tip positions for  $K_{\max}$  and  $K_{\min}$  loading conditions: (a) original crack at maximum crack opening, and (b) at minimum opening (Fig. 6, curve I), (c,d) crack closure immediately after crack is filled with infiltrant (curve II), (e,f) following crack growth through the infiltrant, which is accompanied by onset of a bimodal compliance curve (curve III), and (g,h) after crack growth past the infiltrant, which is accompanied by diminished crack-tip shielding from artificial crack closure (curve IV).

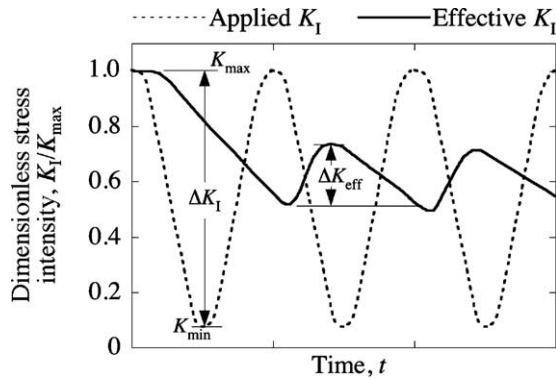


Fig. 10. Reduced effective crack-tip stress intensity due to hydrodynamic pressure from a viscous fluid-filled crack (adapted from Yi et al. [38]). Note: The effective and applied  $K_I$  are both equal to  $K_{\max}$  at  $t = 0$  until viscous damping produces the steady-state condition in the second cycle.

growth rate, with greater potential for brittle polymers ( $n = 4.5\text{--}10$ ), as demonstrated in the current work.

## 5. Conclusions

Experiments were performed to elucidate mechanisms of fatigue crack growth retardation and arrest in microcapsule-toughened epoxy. A protocol based on fatigue life-extension was established for measuring crack healing efficiency under cyclic loading. Fatigue life-extension was achieved by a combination of crack-tip shielding mechanisms. Viscous flow of the healing agent in the crack plane retarded the crack growth process. Polymerization of the healing agent led to a short term adhesive effect and a long term crack closure effect, which prevented full unloading of the crack tip. Significant fatigue-crack retardation was achieved by artificial crack closure induced by a polymerized healing agent (DCPD) wedge at the crack tip that prevented full crack-tip unloading. Moreover, successful crack closure was independent of the adhesive strength of the interface. Crack closure from the polymer wedge continued to retard crack growth long after the crack started to propagate through the healed region.

The mechanisms for retardation and repair associated with manual injection represent the first steps towards a new crack healing methodology. Further development of this methodology is presented in Part II of this paper [33] where retardation and repair of fatigue cracks is achieved through in situ self-healing.

## Acknowledgments

The authors gratefully acknowledge support from the AFOSR Aerospace and Materials Science Directorate

Mechanics and Materials Program (Award No. F49620-02-1-0080), the National Science Foundation (NSF CMS0218863), and Motorola Labs, Motorola Advanced Technology Center, Schaumburg Ill. The authors also thank Profs. J.S. Moore and P.H. Geubelle of the University of Illinois and Dr. A. Skipor of Motorola Labs for technical support and helpful discussions.

## References

- [1] Skibo MD, Hertzberg RW, Manson JA, Kim SL. On the generality of discontinuous fatigue growth in glassy polymers. *J Mater Sci* 1977;12(3):531–42.
- [2] Radon JC. Fatigue growth in polymers. *Int J Fract* 1980;16(6):533–51.
- [3] Sauer JA, Richardson GC. Fatigue of polymers. *Int J Fract* 1980;16(6):499–532.
- [4] Szabo JS, Gryshchuk O, Karger-Kocsis J. Fatigue crack propagation behavior of interpenetrating vinyl ester/epoxy resins. *J Mater Sci Lett* 2003;22(16):1141–5.
- [5] Kawaguchi T, Pearson RA. The moisture effect on the fatigue crack growth of glass particle and fiber reinforced epoxies with strong and weak bonding conditions. Part 2. A microscopic study on toughening mechanism. *Comp Sci Technol* 2004;64(13–14):1991–2007.
- [6] Nagasawa M, Kinuhata H, Koizuka H, Miyamoto K, Tanaka T, Kishimoto H, et al. Mechanical fatigue of epoxy resin. *J Mater Sci* 1995;30(5):1266–72.
- [7] Karger-Kocsis J, Friedrich K. Microstructure-related fracture toughness and fatigue crack growth behavior in toughened, anhydride-cured epoxy resins. *Comp Sci Technol* 1993;48(1–4):263–72.
- [8] Becu L, Maazouz A, Sautereau H, Gerard JF. Fracture behavior of epoxy polymers modified with core-shell rubber particles. *J Appl Polym Sci* 1997;65(12):2419–31.
- [9] Rey L, Poisson N, Maazouz A, Sautereau H. Enhancement of crack propagation resistance in epoxy resins by introducing poly(dimethylsiloxane) particles. *J Mater Sci* 1999;34(8):1775–81.
- [10] Hayes BS, Seferis JC. Modification of thermosetting resins and composites through preformed polymer particles: a review. *Polym Compos* 2001;22(4):451–67.
- [11] Azimi HR, Pearson RA, Hertzberg RW. Role of crack-tip shielding mechanisms in fatigue of hybrid epoxy composites containing rubber and solid glass spheres. *J Appl Polym Sci* 1995;58(2):449–63.
- [12] Sautereau H, Maazouz A, Gerard JF, Trotignon JP. Fatigue behavior of glass bead filled epoxy. *J Mater Sci* 1995;30(7):1715–8.
- [13] McMurray MK, Amagi S. The effect of time and temperature on flexural creep and fatigue strength of a silica particle filled epoxy. *J Mater Sci* 1999;34(23):5927–36.
- [14] Brown EN, White SR, Sottos NR. Fatigue crack propagation in microcapsule toughened epoxy. *J Mater Sci* 2005; in review.
- [15] Azimi HR, Pearson RA, Hertzberg RW. Fatigue of hybrid epoxy composites: epoxies containing rubber and hollow glass spheres. *Polym Eng Sci* 1996;36(18):2352–65.
- [16] Paris PC, Gomez MP, Anderson WE. A rational analytic theory of fatigue. *Trend Eng, Univ Washington* 1961;13(1):9–14.
- [17] Brown EN, White SR, Sottos NR. Microcapsule induced toughening in a self-healing polymer composite. *J Mater Sci* 2004;39(5):1703–10.
- [18] Elber W. Fatigue crack closure under cyclic tension. *Eng Fract Mech* 1970;2(1):37–45.
- [19] Elber W. The significance of crack closure. *Damage Tolerance Aircraft Struct* 1971;ASTM STP 486:230–42.

- [20] Ur-Rehman A, Thomason PF. The effect of artificial fatigue-crack closure on fatigue-crack growth. *Fatig Fract Eng Mater Struct* 1993;16(10):1081–90.
- [21] Song PS, Hwang S, Shin CS. Effect of artificial closure materials on crack growth retardation. *Eng Fract Mech* 1998;60(1):47–58.
- [22] Sharp PK, Clayton JQ, Clark G. Retardation and repair of fatigue cracks by adhesive infiltration. *Fatig Fract Eng Mater Struct* 1997;20(4):605–14.
- [23] Shin CS, Huang KC, Li RZ. Artificial retardation of fatigue crack growth by the infiltration of cracks by foreign materials. *Fatig Fract Eng Mater Struct* 1998;21(7):835–46.
- [24] Galvin GD, Naylor H. Effect of lubricants on the fatigue of steel and other metals. *Proc 1964 Inst Mech Eng* 1965;170(3J):56–70.
- [25] Endo K, Okada T, Komai K, Kiyota M. Fatigue crack propagation of steel in oil. *Bull Jpn Soc Mech Eng* 1972;15(89):1316–23.
- [26] Polk C, Murphy W, Rowe C. Determining fatigue crack propagation rates in lubricating environments through the application of a fracture mechanics technique. *Am Soc Lubr Eng (ASLE) Trans* 1975;18(4):290–8.
- [27] Plumbridge WJ. Mechano-environmental effects in fatigue. *Mater Sci Eng* 1977;27(3):197–208.
- [28] Plumbridge WJ, Ross PJ, Parry JSC. Fatigue crack growth in liquids under pressure. *Mater Sci Eng* 1985;68(2):219–32.
- [29] Tzou JL, Suresh S, Ritchie RO. Fatigue crack propagation in oil environments: 1. crack growth behavior in silicone and paraffin oils. *Acta Metall* 1985;33(1):105–16.
- [30] Tzou JL, Hsueh CH, Evans AG, Ritchie RO. Fatigue crack propagation in oil environments: 2. A model for crack closure induced by viscous fluids. *Acta Metall* 1985;33(1):117–27.
- [31] Davis FH, Ellison EG. Hydrodynamic pressure effects of viscous fluid flow in a fatigue crack. *Fatig Fract Eng Mater Struct* 1989;12(6):527–42.
- [32] White SR, Sottos NR, Geubelle PH, Moore JS, Kessler MR, Sriram SR, Brown EN, Viswanathan S. Autonomic healing of polymer composites. *Nature* 2001;409(6822):794–7.
- [33] Brown EN, White SR, Sottos NR. Retardation and repair of fatigue cracks in a microcapsule toughened epoxy composite – Part II: In situ self-healing. *Comp Sci Tech* 2005;65 in review.
- [34] Brown EN, Kessler MR, Sottos NR, White SR. In situ poly(urea-formaldehyde) microencapsulation of dicyclopentadiene. *J Microencap* 2003;20(6):719–30.
- [35] Brown EN, Sottos NR, White SR. Fracture testing of a self-healing polymer composite. *Exp Mech* 2002;42(4):372–9.
- [36] Mostovoy S, Crosley PB, Ripling EJ. Use of crack-line loaded specimens for measuring plane-strain fracture toughness. *J Mater* 1967;2(3):661–81.
- [37] Simon SL, McKenna GB, Sindt O. Modeling the evolution of the dynamic mechanical properties of a commercial epoxy during cure after gelation. *J Appl Polym Sci* 2000;76(4):495–508.
- [38] Yi KS, Cox BN, Dauskardt RH. Fatigue crack-growth behavior of materials in viscous fluid environment. *J Mech Phys Solid* 1999;47(9):1843–71.